

Accepted Manuscript

Discovery and evaluation of the hybrid of bromophenol and saccharide as potent and selective protein tyrosine phosphatase 1B inhibitors

Renshuai Zhang, Rilei Yu, Qi Xu, Xiangqian Li, Jiao Luo, Bo Jiang, Lijun Wang, Shuju Guo, Ning Wu, Dayong Shi



PII: S0223-5234(17)30258-1

DOI: [10.1016/j.ejmech.2017.04.004](https://doi.org/10.1016/j.ejmech.2017.04.004)

Reference: EJMECH 9351

To appear in: *European Journal of Medicinal Chemistry*

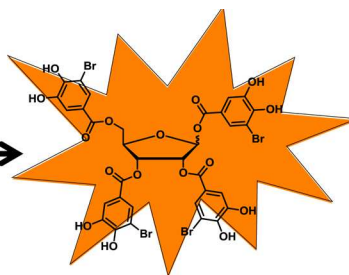
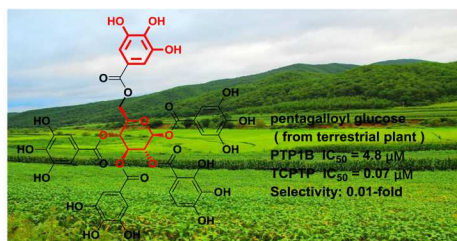
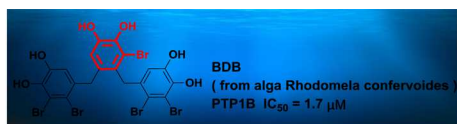
Received Date: 1 February 2017

Revised Date: 21 March 2017

Accepted Date: 2 April 2017

Please cite this article as: R. Zhang, R. Yu, Q. Xu, X. Li, J. Luo, B. Jiang, L. Wang, S. Guo, N. Wu, D. Shi, Discovery and evaluation of the hybrid of bromophenol and saccharide as potent and selective protein tyrosine phosphatase 1B inhibitors, *European Journal of Medicinal Chemistry* (2017), doi: 10.1016/j.ejmech.2017.04.004.

This is a PDF file of an unedited manuscript that has been accepted for publication. As a service to our customers we are providing this early version of the manuscript. The manuscript will undergo copyediting, typesetting, and review of the resulting proof before it is published in its final form. Please note that during the production process errors may be discovered which could affect the content, and all legal disclaimers that apply to the journal pertain.



PTP1B $IC_{50} = 0.19 \mu M$
TCP1P $IC_{50} = 5.94 \mu M$
Selectivity: 32-fold
showed appropriate permeability
and cellular activity

ACCEPTED MANUSCRIPT

Discovery and evaluation of the hybrid of bromophenol and saccharide as potent and selective Protein tyrosine phosphatase 1B inhibitors

Renshuai Zhang,^{ab} Rilei Yu,^d Qi Xu,^{ab} Xiangqian Li,^{ab} Jiao Luo,^{ab} Bo Jiang,^{ab} Lijun Wang,^{ab} Shuju Guo,^{ab} Ning Wu,^{ab} Dayong Shi^{*abc}

^aKey Laboratory of Experimental Marine Biology, Institute of Oceanology, Chinese Academy of Sciences, Qingdao, China.

^bLaboratory for Marine Drugs and Bioproducts, Qingdao National Laboratory for Marine Science and Technology, Qingdao, China.

^cUniversity of Chinese Academy of Sciences, Beijing, China.

^dKey Laboratory of Marine Drugs, The Ministry of Education of China, School of Medicine and Pharmacy, Ocean University of China, Qingdao 266003, China.

*Corresponding author: Tel. +86-0532-8289-8719; Fax: +86-0532-8289-8741; E-Mail: shidayong@qdio.ac.cn.

Abstract

Protein tyrosine phosphatase 1B (PTP1B) is a key negative regulator of insulin signaling pathway. Inhibition of PTP1B is expected to improve insulin action. Appropriate selectivity and permeability are the gold standard for excellent PTP1B inhibitors. In this work, molecular hybridization-based screening identified a selective competitive PTP1B inhibitor. Compound **10a** has IC₅₀ values of 199 nM against PTP1B, and shows 32-fold selectivity for PTP1B over the closely related phosphatase TCPTP. Molecule docking and molecular dynamics studies reveal the reason of selectivity for PTP1B over TCPTP. Moreover, the cell permeability and cellular activity of compound **10a** are demonstrated respectively.

Key words: PTP1B; bromophenol; saccharide; selectivity; permeability

Introduction

Diabetes mellitus is a comprehensive metabolic syndrome, with the progress of the disease, which may lead to blurring vision, cardiovascular diseases, kidney or other organ damage, dysfunction and many more.[1] Type-II diabetes accounts for more than 90% of the total in all diabetics.[2] PTP1B down regulates insulin signaling by catalyzing the dephosphorylation of phosphotyrosine residues, and precise control of

the phosphorylation levels of proteins involved in insulin signal pathways.[3, 4] Elchebly, M. and Klamon, L. D. et al have disclosed that PTP1B knockout mice revealed phenotypes of enhanced sensitivity to insulin, lower plasma glucose and insulin levels in 1999 and 2000.[5, 6] Thus, PTP1B was recognized as an attractive therapeutic target for type-II diabetes.[7] PTP1B was the first validated PTP target, which has been cloned and fully characterized in 1988. However, as of 2016, there were not any of small molecule PTP1B inhibitors, as therapeutic drug for type-II diabetes, approved over the world. This is in sharp contrast to that several small molecule kinase inhibitors have been approved in recent years.[8] Why is this so?

Three significant challenges to the development of excellent small molecule PTP1B inhibitors are: (1) the relatively shallow nature of the catalytic pocket of PTP1B, which is disadvantageous for binding of small molecule inhibitors.[9] (2) the catalytic pocket consists of several polar amino acids (Ser216, Cys215 and Arg221 et al), which result in that small molecules only containing polar groups could effectively bind to the catalytic site.[10] The initial PTP1B inhibitors were pTyr mimetics based on the electrostatic properties of active site. The phosphonates, carboxylic acids, sulphonamides and sulphanamic acids were initially used as pTyr mimetics for designing of PTP1B inhibitors.[11-13] These pTyr mimetics with negative charge were hydrophilic, which resulted in poor cell permeability and oral bioavailability. (3) TCPTP is the most homologous to PTP1B, with 74% sequence identity in the catalytic region. However, the knockout of TCPTP would result in abnormalities in B cell and T cells functions.[14] Therefore, it is difficult but important to achieve high selectivity for PTP1B over TCPTP based on above observation.

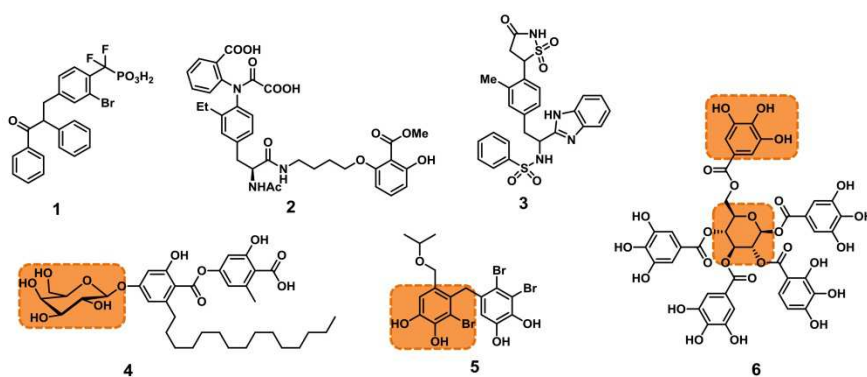


Figure 1. Structures of PTP1B inhibitors

A number of PTP1B inhibitors including synthetic and natural small molecules have been discovered and structure-based design (**Fig 1**).[15-18] Compound **1**, **2** and **3** were classic PTP1B inhibitors, which were designed on the basis of catalytic pocket characteristics. Compound **4**, **5** and **6** were derived from natural products and have also been proved to be active against PTP1B. The compound **1** and 2-oxalylarylamino benzoic acid derivative **2** showed potent activity (**1** : $IC_{50}=120$ nM,

2: $IC_{50} = 18$ nM). Unfortunately, they showed little selectivity (**1**: 1.0-fold; **2**: 3.6-fold) for PTP1B over TCPTP.[19, 20] The compound **3** was a heterocyclic pTyr Mimetic without electronegative groups, showed nanomolar activity ($IC_{50}=32$ nM) and demonstrated modest caco-2 permeability (0.4×10^{-6} cm/s), but without selectivity.[15, 21, 22] Additionally, a number of PTP1B inhibitors from natural product have also been discovered. The natural products **4**, **5** and **6** exhibited a micromolar level of activity (**4**: $IC_{50} = 0.18$ μ M; **5**: $IC_{50} = 2.42$ μ M; **6**: $IC_{50} = 4.8$ μ M) against PTP1B, however, the selectivity or membrane permeability of these compounds were not further reported.[23-25] All of above observations indicated that (1) some PTP1B inhibitors derived from plants or microorganism without charged groups only showed modest activity, (2) some artificially designed inhibitors exhibited excellent inhibitory activity, but lacked adequate membrane permeability or selectivity. It is relatively easy to obtain highly active PTP1B inhibitors. The real greater challenge is to enhance the selectivity and permeability of PTP1B inhibitors.

Our laboratory has reported a number of bromophenols (BPN, BDB et al) derived from marine *alga Rhodomela confervoides*, which displayed sub-micromolar PTP1B activity.[26-31] They shared similar structural features, that was, containing one or more bromophenol functional groups. Similarly, a large number of polyphenols have also been found in terrestrial plants, which showed a variety of biological activity, including anti-parasite, antitumor, antioxidant, antibacterial and anti-diabetic.[25, 32-35] Unlike natural products derived from the sea, terrestrial plant metabolites are usually free of halogens because of the lack of halogen sources. Pentagalloyl glucose was discovered in roots and fruits of a variety of terrestrial plants, which showed micromolar activity against PTP1B, but without further study of selectivity and permeability.[25, 36] Would it work if polyphenols derived from terrestrial plants were replaced by bromophenols from marine algae? The initial design strategy of these hybrid molecules was shown in **Fig S1**.

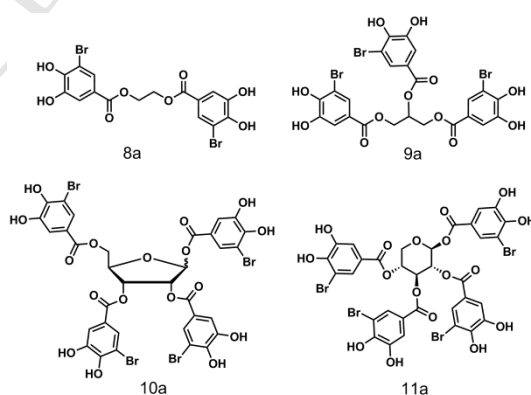


Figure 2. Compounds **8-11a** were first designed.

Compound **10a** and **11a** were originally designed, which incorporated four molecules of bromophenol functional groups that were coupled to ribose or xylose

respectively. In order to investigate the effect of number of functional groups on activity, compounds **8a** and **9a** were also designed (**Fig 2**). The synthetic route of title molecules **8-11a** was shown in **Scheme S1**. Interestingly, only β -anomer of **11a** was obtained. The effect of synthesized compounds (**3a-11a**) on recombinant PTP1B inhibition was evaluated using colorimetric assay. The inhibitory rate was measured at concentration of 10 μM , and the compounds with good inhibition rate ($>50\%$ at 10 μM) were selected for IC_{50} assay. The results of the enzymatic assay were shown in **Table 1**. The intermediates (**3a-7a**), which contain one or more bromophenol groups protected by TBDMS, do not exhibit PTP1B inhibitory activity with the inhibition rate $< 50\%$ at 10 μM . The targeted compounds (**9a-11a**) with 3 or 4 bromophenol groups are ideal to potent inhibitors of PTP1B with IC_{50} values 0.19-0.24 μM . The compound **8a**, with two bromophenol groups coupled by ethylene glycol, is significantly less active toward PTP1B. Interestingly, the increase of bromophenol group leads to enhanced compound activity, whereas the xylose or ribose linker has little effect on activity. Does an analog containing 5 bromophenol groups have the higher activity? Unfortunately, we failed to synthesize glucose bromophenol derivatives, which contain 5 bromophenol groups and coupled by glucose. That was probably due to the presence of bromine atoms which greatly increased the steric hindrance. Additionally, the compound **6** (**Fig 1**) with five polyphenol groups coupled by glucose, showed IC_{50} value of 4.8 μM against PTP1B. The activity of **9-11a** was 20-fold greater than that of **6**.

Table 1. Inhibition of PTP1B by Inhibitors **3-11a**

compd	% PTP1B inhibition (at 10 μM)	IC_{50} (μM)	compd	% PTP1B inhibition (at 10 μM)	IC_{50} (μM)
3a	24.23 \pm 3.00	-	8a	25.04 \pm 6.33	-
4a	32.83 \pm 3.24	-	9a	95.45 \pm 11.20	0.24 \pm 0.02
5a	12.02 \pm 5.43	-	10a	96.37 \pm 9.76	0.19 \pm 0.04
6a	43.56 \pm 5.86	-	11a	99.00 \pm 15.38	0.20 \pm 0.03
7a	41.94 \pm 10.32	-	6^a		4.8

^a**6**: data from literature.[25]

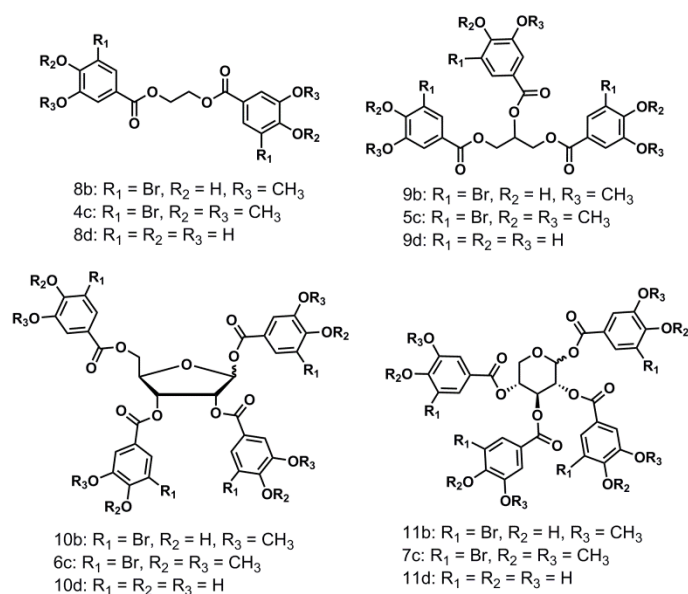


Figure 3. Compounds were designed for SAR study.

To investigate the effect of phenolic hydroxyl and bromine atoms on the activity, analogues (**8-11b**, **4-7c**, **8-11d**) bearing varying substituted benzene ring were prepared (**Fig 3**). The structures and synthetic route of these compounds were shown in **Scheme S2**. The compounds **11b** and **11d** were β -anomer, which was same to that of **11a**. However, α and β -anomer of **7c** were obtained under the same condition. These new analogues were then evaluated for their ability to inhibit PTP1B in colorimetric assay (**Table 2**). The compound **8b**, **4c** and **8d**, containing different substituted benzene rings which were coupled by ethylene glycol, showed no activity ($IC_{50} > 20 \mu M$). The observation was consistent with compound **8a**, which revealed that compounds containing two bromophenol groups did not have PTP1B inhibitory activity. Compound **9b**, one of the hydroxyl groups on every substituted benzene ring was replaced by a methoxy group, showed modest inhibition against PTP1B ($IC_{50} = 8.45 \mu M$). However, the activity of compound **9b** is significantly decreased compared with the corresponding compound **9a**, which contains two hydroxyl groups on every substituted benzene ring. Further, the compound **5c**, all hydroxyl groups were replaced by methoxy groups, was completely inactive against PTP1B. The same conclusion was observed for compounds **10a**, **10b**, **6c** and **11a**, **11b**, **7c**. It revealed that the compounds with free hydroxyl groups were more potent PTP1B inhibitors than the corresponding methoxyl compounds. The compounds **10b** and **6c** displayed obvious improvement in potency compared with the corresponding compounds **9b** and **5c**, and it is consistent to that the PTP1B inhibitory activity of **10a** is greater than **9a**. It indicated that the increase of bromophenol group improved PTP1B inhibitory activity. The compound **9d** containing 3, 4-dihydroxybenzene ring exhibited weaker activity than that of compound **9a** and **9b** bearing bromine-substituted benzene ring. It

was similar that the inhibitor **10d** and **11d** showed higher IC_{50} values than **10a** and **11a**, respectively. Reduction of bromine atom led to drop in PTP1B inhibitory potency, suggested that the existence of bromine substitution on the phenyl ring had a certain influence on the inhibitory activity against PTP1B. It was unclear why inhibitor **7c** and **11b** were more active than the closely related inhibitors **6c** and **10b**, on the contrast, the compound **11d** and **11a** were less active than **10d** and **10a**. It was ambiguous that the effect of saccharide on activity against PTP1B. In general, compound **10a** bearing dihydroxy bromobenzene group exhibited the best inhibitory activity and was selected for further study.

Table 2. Inhibition of PTP1B by Inhibitors **8-11b**, **4-7c**, **8-11d**

compd	IC_{50} (μ M)	compd	IC_{50} (μ M)
8b	> 20	6c	3.41 ± 0.13
9b	8.45 ± 0.11	7c	1.11 ± 0.08
10b	1.50 ± 0.13	8d	> 20
11b	0.75 ± 0.06	9d	12.3 ± 0.26
4c	> 20	10d	2.20 ± 0.22
5c	> 20	11d	3.00 ± 0.32

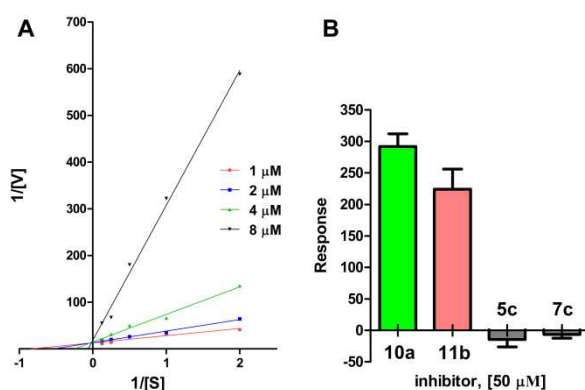


Figure 4. (A) Compound **10a** is a classical competitive inhibitor. (B) Interaction of inhibitors (**10a**, **11b**, **5c** and **7c**) with PTP1B by SPR. Data is presented as maximum binding.

A detailed kinetic analysis of **10a** was then conducted using p-NPP as the small-molecule substrate in a continuously monitored colorimetric assay. Lineweaver-Burk analyses of compound **10a** against PTP1B, confirmed that it was a competitive inhibitor with classical kinetic behavior (**Fig 4A**). The surface plasmon resonance (SPR) could characterize the interaction between drug targets and small-molecules and has been exploited as a powerful tool for drug discovery. Here,

the SPR technology was used to analyse small molecule (**10a**, **11b**, **5c** and **7c**) binding to PTP1B. SPR traces were presented in **Fig S2**. The response values of representative inhibitors were displayed in **Fig 4B**. The compound **10a** contained two phenolic hydroxyl in one bromophenol functional group showed most potent binding to PTP1B. The inhibitor **11b** bearing a phenolic hydroxyl in one bromophenol group showed a significant reduction in binding to PTP1B. Conversely, no binding was observed in compounds **5c** and **7c** which did not contain free phenolic hydroxyl groups. Additionally, the inhibitors (**10a**, **11b**, **5c** and **7c**) displayed no binding to the blank (**Fig S3**), in which there was no immobilized protein. The SPR binding data demonstrated that the compound **10a** could be bond to PTP1B and supported an important role for phenolic hydroxyl in the interaction with PTP1B.

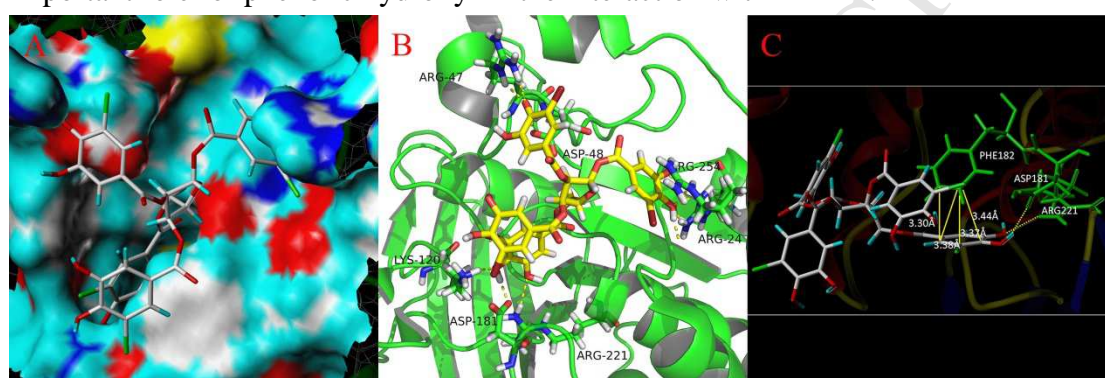


Figure 5. Model of inhibitor **10a** bound to PTP1B (PDB: 1QXK). (A) The surface of catalytic pocket of PTP1B. (B) H-bonds between **10a** and key amino acids. (C) The distance between PHE182 and **10a**.

Molecular docking was performed to predict the binding mode of **10a** with PTP1B and explain the interaction of **10a** with PTP1B. The X-ray structure of PTP1B with a difluorophosphate inhibitor as the ligand was used as the starting point (PDB code 1QXK).[37] After the difluorophosphate inhibitor was removed from the protein structure, **10a** was minimized using Tripos force field of SYBYL-X 2.0 software. **Fig 5A** showed the binding orientation of **10a** minimized in the catalytic binding pocket of PTP1B. The binding site of the PTP1B was shown in the opaque molecular surface colored by atom type representation. One of the substituted benzene ring was embedded into the catalytic pocket, and the remaining substituted benzene rings were located at the inlet of the catalytic pocket. The dihydroxybenzene ring moiety plays an important role in the binding, as a plurality of hydroxyl groups involved in hydrogen bonding interactions with amino acid residues Lys120, Asp181 and Arg47, 48, 221 et al (**Fig 5B**). The key distance (3.30 - 3.44 Å) between a substituted benzene ring which was not involved in the formation of H-bonds and Phe182 was shown in **Fig 5C**. A π - π stacking interaction was observed between the phenyl ring and Phe182. All of the substituted benzene rings of inhibitor **10a** formed an interaction with

corresponding amino acid residues, that might explain why compound **10a** exhibited excellent activity against PTP1B.

Table 3. Inhibition of Phosphatases by Inhibitors **9a** and **10a**

compd	IC ₅₀ (μM)				Selective ^b
	PTP1B	TCPTP	SHP2	PTPLAR	
9a	0.24 ± 0.02	1.98	4.53	NA ^a	8.0
10a	0.19 ± 0.04	5.94	15.86	NA	32.0
6^c	4.8	0.07	> 50	> 50	0.01

^aNA: no activity (the inhibitor % in 20 μg/mL < 25.0%). ^bSelective: IC₅₀ (TCPTP)/IC₅₀ (PTP1B). ^c**6**: data from literature.[25]

Compound **10a** is the best inhibitor in all title compounds against PTP1B. Does it have selectivity for PTP1B over other phosphatases? Further, the selectivity of the **9a** and **10a** was determined by measuring their inhibitory activity against a panel of several phosphatases including TCPTP, SHP-2 and PTPLAR. The IC₅₀ values of inhibitors **9a** and **10a** against the phosphatases, and the selectivity ratios were shown in **Table 3**. The compound **9a** and **10a** showed no activity against PTPLAR, and only exhibited moderate activity for SHP2. We were gratified to find that compound **9a** and **10a** were selective for PTP1B over PTPLAR and SHP2. On the basis of amino acid sequence homology, TCPTP was the phosphatase most closely related to PTP1B. The inhibitor **9a** had 8-fold selectivity for PTP1B over TCPTP. Furthermore, the compound **10a** showed 32-fold selectivity for PTP1B over TCPTP. It was a significant level of selectivity given the 74% sequence homology in their catalytic active site. The compound **10a** was more excellent than the vast majority of PTP1B inhibitors reported in literatures.[15, 16, 38] Additionally, the compound **6** did not exhibit selectivity for PTP1B over TCPTP, by contrast, displayed the lower IC₅₀ value against TCPTP than that of PTP1B.

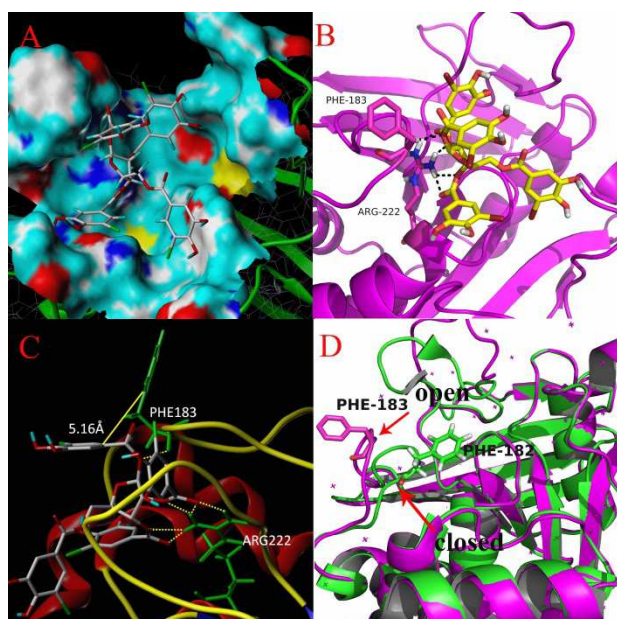


Figure 6. (A), (B) and (C): The binding mode and interactions of compound **10a** with TCPTP (PDB: 1L8K). The surface of catalytic pocket of TCPTP, the key amino acids and the distance between Phe183 and **10a** are shown separately. (D) The structure of TCPTP (pink) has been aligned with PTP1B (green).

A positive effort was made to explain the selectivity of inhibitor **10a** by performing molecular docking and molecular dynamics (MD) simulations. The binding mode of compound **10a** with TCPTP [39] was displayed in of **Fig 6A**. Some main interactions between inhibitor **10a** and the receptor can be observed in of **Fig 6B** and **6C**. The superimposed images of secondary structures of TCPTP and PTP1B (PDB: 1QXK) was shown in of **Fig 6D**, as the Phe182 of PTP1B and Phe183 of TCPTP were displayed separately. Only one crystal structure of TCPTP was available in the Protein Data Bank, and this structure has the WPD loop in the open position, which formed a larger catalytic pocket than that of PTP1B. The substituted benzene rings were loosely distributed in the binding pocket. Only the oxygen atoms of the ribose and the ester bonds formed hydrogen bonding with amino acid residues Arg222 and Phe183, that was different from the binding pattern of **10a** with PTP1B (**Fig 5A** and **5B**). In addition, in contrast to the closed WPD loop of PTP1B, the WPD loop of TCPTP is open, which led to the opposite orientation of Phe183 (**Fig 6D**). The closest distance between the substituted benzene ring and Phe183 is 5.16 Å, which resulted in the loss of π - π stacking or T-shape interaction.

Unlike the only TCPTP structure with an open WPD loop did not bind with any ligands, the PTP1B (PDB: 1QXK) with a closed WPD loop had a difluorophosphonate inhibitor as the ligand. A ligand-free PTP1B crystal structure (PDB: 3A5J) was chosen for further investigation of the mode of binding to the

inhibitor **10a**, considering that the presence of the ligand might affect the position of loop. The binding mode and H-bond interaction were shown in **Fig S4**. The orientation of **10a** in binding pocket of PTP1B (PDB: 3A5J) was very similar to that in TCPTP (**Fig 6A**). However, there are three substituted benzene rings of compound **10a** that formed H-bonds with PTP1B (**Fig S4B**), which was completely different from the bonding between **10a** and TCPTP. Although the WPD loop of PTP1B (PDB: 3A5J) without ligands was also in the open position which was the same to TCPTP, the orientation of Phe182 in PTP1B (PDB: 3A5J) showed a significant difference with that of Phe183 in TCPTP (**Fig. S5A**). Most notably, the distance between Phe182 and one of substituted benzene ring was appropriate for the formation of π - π stacking interaction (**Fig. S5B**).

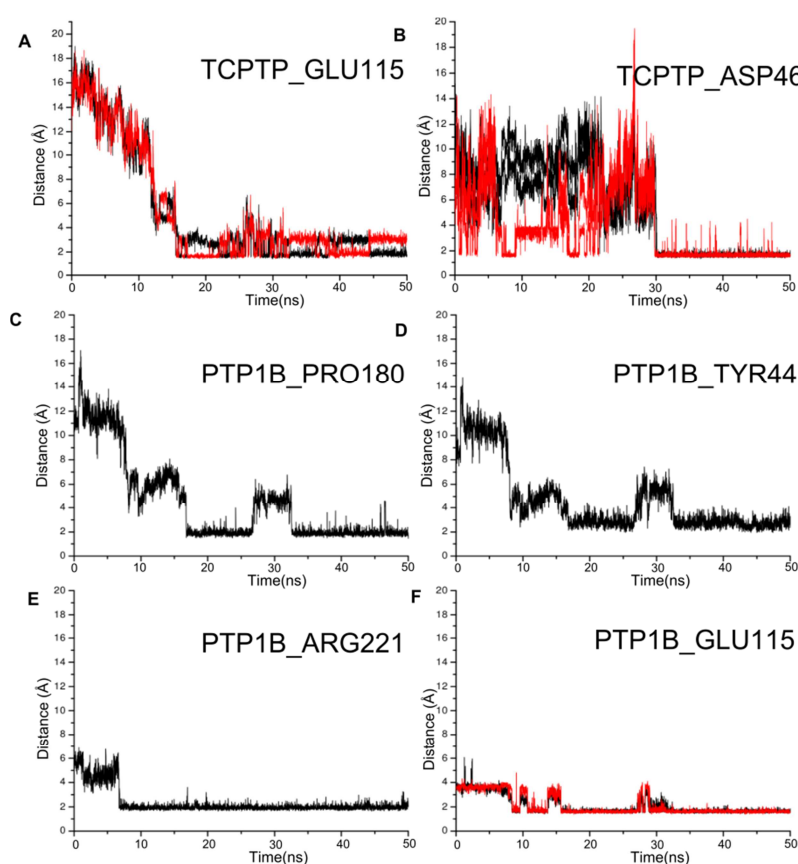


Figure 7. Evolution of the distance between the pairwising interacting atoms that can form H-bonds from **10a** and residues of TCPTP (1L8K) or PTP1B (3A5J).

The interaction of the protein with ligands is a dynamic process that results in a lower binding energy of the complex and a more stable complex. Molecular docking is a static process, it can only show the interaction of ligand and protein at a certain moment. While the dynamic process of ligand-protein binding could be displayed by MD simulation, which take into account the influence of water molecules and ions et al. The binding modes of **10a** and PTP1B (3A5J) or TCPTP (1L8K) were shown in

Fig S6 after 50 nanoseconds of MD simulation. Compound **10a** bound with the TCPTP and PTP1B in a similar mode with three aromatic rings embedded into the binding site and the fourth one exposed outside. Three benzene rings of **10a** were loosely distributed in the binding pocket of TCPTP, whereas the three benzene rings embedded in PTP1B form π - π stacking interaction which made the ligand more stable. Further, the hydroxyl groups at the aromatic ring formed hydrogen bonds with Glu115 and Asp46 of TCPTP, whereas four amino acids were involved in the interaction between the PTP1B and inhibitor **10a**. The H-bonds between Glu115, Asp46 and inhibitor **10a** were newly generated during MD simulation, and the original interactions between Phe183, Arg22 and **10a** were lost in complex TCPTP/**10a** (**Fig 6B** and **Fig S6A**). The H-bonds between Glu115, Arg222 and the inhibitor were always present throughout the MD simulation in complex PTP1B/**10a** (**Fig S4B** and **Fig S6B**). The stability of these hydrogen bonds was evaluated by calculating the evolution of distances between H-bond interacting atoms in 50 ns MD simulations (**Fig 7**). The distances of the pairwise interacting residues substantially fluctuated at the beginning of the MD except that between Glu115, Arg222 and **10a** in complex PTP1B/**10a**. Afterwards, the distances reached equalization and maintained constant in the last 20 ns of the MD, which suggested that these hydrogen bonds were stable. Additionally, the distance between benzene rings of **10a** and phenylalanine of PTP1B or TCPTP was more than 5 Å, which resulted in the loss of π - π stacking or T-shape interaction (**Fig S7**). The observation was different from the result found in molecule docking (**Fig 5C** and **Fig S5B**), and indicated that the interaction of the ligand with phenylalanine was unstable and not durable.

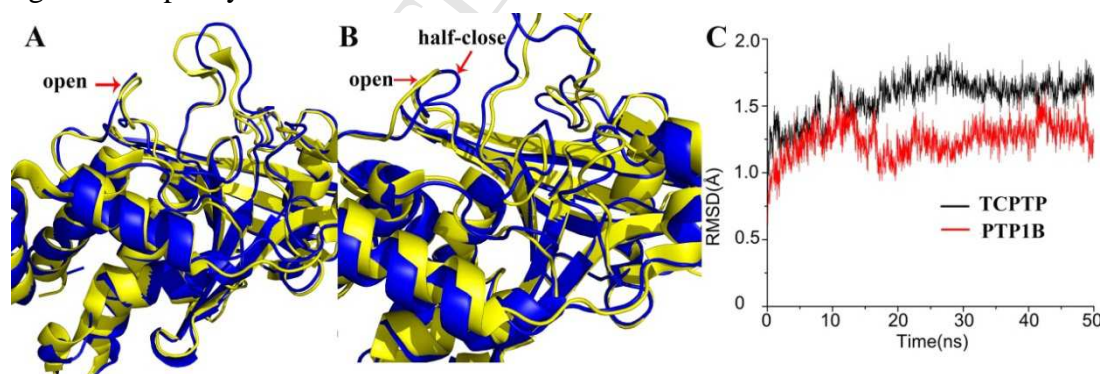


Figure 8. (A) PTP1B (3A5J, in yellow) was aligned with itself after dynamic simulation (in blue). (B) TCPTP (1L8K, in yellow) was aligned with itself after dynamic simulation (in blue). (C) Molecular dynamic simulation of **10a** bound with TCPTP (1L8K, in black) and PTP1B (3A5J, in red).

The change of protein conformation reflects its stability in MD simulation. The WPD loop is highly correlated with the catalytically active site of PTP1B and TCPTP. The WPD loop of PTP1B (3A5J) has always been in open position before and after

dynamic simulation (**Fig 8A**), in contrast, the position of loop of TCPTP (1L8K) changes from open to half-close (**Fig 8B**). The root-mean-squared deviation (RMSD) is widely used to assess the distance between two aligned objects. The backbone RMSD value of PTP1B was lower than that of TCPTP, which suggested that the PTP1B/**10a** was more stable than TCPTP/**10a** in 50 ns MD simulation (**Fig 8C**). All the above observations suggested that the interaction between **10a** and PTP1B was more potent and stable than that between **10a** and TCPTP. That may be the reason, at least in part, why the compound **10a** displayed significant selectivity for PTP1B over TCPTP.

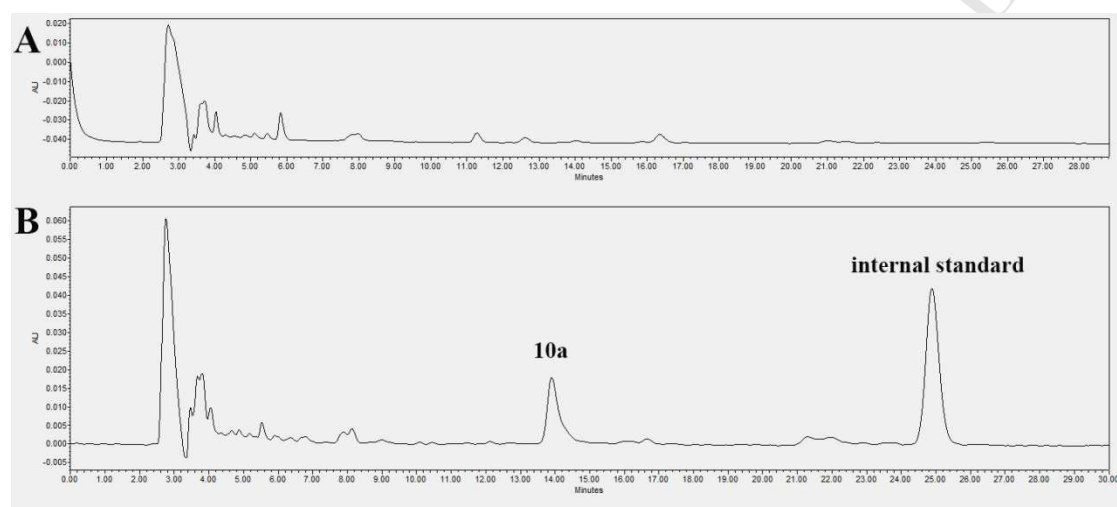


Figure 9. Cell uptake of compound **10a** in C2C12 myotubes (10 μ M exposure for 8 h). (A) DMSO treat group (control). (B) The internal standard (10 mM \times 10 μ L) was added after cell was disrupted.

The permeability of inhibitor **10a** was assayed in C2C12 myotubes by HPLC (**Fig. 9**). Cell was treated with DMSO (control group) or **10a** (0.1 μ mol) and subsequently incubated for 8 h. The medium was then removed and cell was disrupted. An equal amount of the internal standard[40] was added, and then the cell debris was removed by filtration. The amount of compound **10a** ingested into the cell was analyzed by HPLC to obtain cell uptake. The result suggested that the proportion of compound **10a** ingested into the cells was about 36.9%. Approximately 74.0 pmmol of compound **10a** could be absorbed per million cells, which was considered to be an appropriate degree of cell uptake.[41]

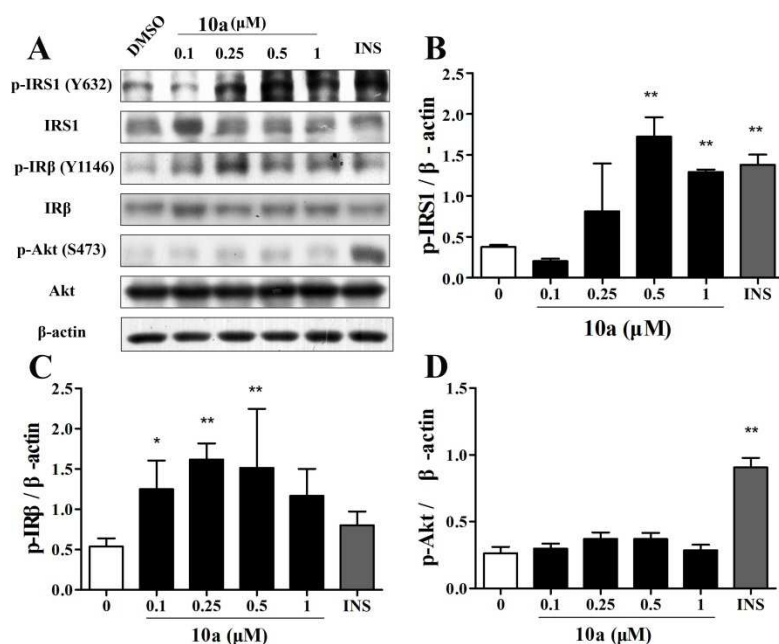


Figure 10. (A) Activation of insulin signaling during exposure of C2C12 myotubes to **10a**. C2C12 myotubes were treated with **10a** or 100 nM insulin. (B), (C) and (D) Phosphorylation levels of IRS1, IR β and Akt. Band density was quantified and normalized with β -actin. The results shown are means \pm SD (n = 3). (* P < 0.05, ** P < 0.01 versus DMSO-treated group)

To determine the molecular mechanism underlying the effects of inhibitor **10a** on insulin signaling, the total and phosphorylated protein expression levels were performed by western blotting. Protein band intensities were quantified by densitometric analysis. The result showed that compound **10a** (0.25, 0.5 and 1.0 μ M) increased p-IRS1 expression in an insulin-independent manner (**Fig. 10**). Inhibitor **10a** also significantly increased the relative abundances of p-IR β and p-Akt compared with that in the control group (DMSO-treated) without affecting the expression levels of total IR β and Akt. The results demonstrated that compound **10a** activates insulin signaling through up-regulating the phosphorylation level of IRS-1, IR β and Akt.

Conclusion

In summary, the incorporation of bromophenol functional groups derived from marine algae and saccharide by simple molecular hybridization led to the discovery of some PTP1B inhibitors. Inhibitor **10a**, which incorporated bromophenol and ribose, emerged as the most potent PTP1B inhibitor in all targeted compounds with IC₅₀ values of 199 nM and 32-fold selectivity over TCPTP. Molecular modeling and SPR studies indicated that the phenolic hydroxyls in benzene rings played an important role in the interaction of inhibitors and PTP1B. The MD studies revealed that the

PTP1B/**10a** complex was more stable than TCPTP/**10a**, which was the potent proof for observed 32-fold selectivity of **10a** for PTP1B over TCPTP, although TCPTP and PTP1B shared high degree of homology in catalytic site. Additionally, the moderate permeability of inhibitor **10a** was directly demonstrated by HPLC. Moreover, **10a** displayed cellular activity in an IR phosphorylation assay. These results provided further evidence that bromophenol compounds incorporating saccharides can be potent inhibitors of PTP1B. Further studies on these compounds in cell permeability, selectivity and cellular activity would be necessary to provide PTP1B inhibitors suitable for in vivo proof of animal studies in diabetes.

Acknowledgements

This work was supported by the National Natural Science Foundation of China (No. 41506169), and Key research and development project of Shandong province (2015GSF115029, 2016ZDJS07A13), and the Project of Discovery, Evaluation and Transformation of Active Natural Compounds, Strategic Biological Resources Service Network Programme of Chinese Academy of Sciences (ZSTH-026), and the Scientific and Technological Innovation Project Financially Supported by Qingdao National Laboratory for Marine Science and Technology (No. 2015ASKJ02), and Aoshan Talents Program Supported by Qingdao National Laboratory for Marine Science and Technology (NO. 2015ASTP).

Notes

The authors declare no competing financial interest.

References:

- [1] D.W.C.A. Plotnick. Type 1 Diabetes Mellitus in Pediatrics. *Pediatr. Rev.* 29 (2008), 374-385.
- [2] Diagnosis and Classification of Diabetes Mellitus. *Diabetes Care.* 36 (2012), S67-S74.
- [3] S. Yip, S. Saha, J. Chernoff. PTP1B: a double agent in metabolism and oncogenesis. *Trends Biochem Sci.* 35 (2010), 442-449.
- [4] K.A. Kenner, E. Anyanwu, J.M. Olefsky, J. Kusari. Protein-tyrosine Phosphatase 1B Is a Negative Regulator of Insulin- and Insulin-like Growth Factor-I-stimulated Signaling. 271 (1996), 19810-19816.
- [5] L.D. Klaman, O. Boss, O.D. Peroni, J.K. Kim, J.L. Martino, J.M. Zabolotny, N. Moghal, M. Lubkin, Y.B. Kim, A.H. Sharpe, A. Stricker-Krongrad, G.I. Shulman, B.G. Neel, B.B. Kahn. Increased energy expenditure, decreased adiposity, and tissue-specific insulin sensitivity in protein-tyrosine phosphatase 1B-deficient mice. *Mol Cell Biol.* 20 (2000), 5479-5489.
- [6] M. Elchebly, P. Payette, E. Michaliszyn, W. Cromlish, S. Collins, A.L. Loy, D. Normandin, A. Cheng, J. Himms-Hagen, C.C. Chan, C. Ramachandran, M.J. Gresser, M.L. Tremblay, B.P. Kennedy. Increased insulin sensitivity and obesity resistance in mice lacking the protein tyrosine

- phosphatase-1B gene. *Science*. 283 (1999), 1544-1548.
- [7] V.S. Murthy, V.M. Kulkarni. 3D-QSAR CoMFA and CoMSIA on protein tyrosine phosphatase 1B inhibitors. *Bioorg Med Chem*. 10 (2002), 2267-2282.
- [8] R. Zhang, S. Chen, X. Zhang, R. Yu, S. Wan, M. Geng, T. Jiang. Synthesis and evaluation of novel non-covalent binding quinazoline glycoside derivatives targeting the L858R and T790M variants of EGFR. *RSC Adv*. 6 (2016), 36857-36862.
- [9] S.L. McGovern, E. Caselli, N. Grigorieff, B.K. Shoichet. A Common Mechanism Underlying Promiscuous Inhibitors from Virtual and High-Throughput Screening. *J Med Chem*. 45 (2002), 1712-1722.
- [10] D. Barford, A.J. Flint, N.K. Tonks. Crystal structure of human protein tyrosine phosphatase 1B. *Science*. 263 (1994), 1397-1404.
- [11] K. Shen, Y.F. Keng, L. Wu, X.L. Guo, D.S. Lawrence, Z.Y. Zhang. Acquisition of a specific and potent PTP1B inhibitor from a novel combinatorial library and screening procedure. *J Biol Chem*. 276 (2001), 47311-47319.
- [12] S. Shrestha, B.R. Bhattarai, K.H. Lee, H. Cho. Mono- and disalicylic acid derivatives: PTP1B inhibitors as potential anti-obesity drugs. *Bioorg Med Chem*. 15 (2007), 6535-6548.
- [13] K.K. Amarasinghe, A.G. Evdokimov, K. Xu, C.M. Clark, M.B. Maier, A. Srivastava, A.O. Colson, G.S. Gerwe, G.E. Stake, B.W. Howard, M.E. Pokross, J.L. Gray, K.G. Peters. Design and synthesis of potent, non-peptidic inhibitors of HPTPbeta. *Bioorg Med Chem Lett*. 16 (2006), 4252-4256.
- [14] K.E. You-Ten, E.S. Muise, A. Itie, E. Michaliszyn, J. Wagner, S. Jothy, W.S. Lapp, M.L. Tremblay. Impaired bone marrow microenvironment and immune function in T cell protein tyrosine phosphatase-deficient mice. *J Exp Med*. 186 (1997), 683-693.
- [15] A.P. Combs, W. Zhu, M.L. Crawley, B. Glass, P. Polam, R.B. Sparks, D. Modi, A. Takvorian, E. McLaughlin, E.W. Yue, Z. Wasserman, M. Bower, M. Wei, M. Rupa, P.J. Ala, B.M. Reid, D. Ellis, L. Gonneville, T. Emm, N. Taylor, S. Yeleswaram, Y. Li, R. Wynn, T.C. Burn, G. Hollis, P.C.C. Liu, B. Metcalf. Potent Benzimidazole Sulfonamide Protein Tyrosine Phosphatase 1B Inhibitors Containing the Heterocyclic (S)-Isothiazolidinone Phosphotyrosine Mimetic. *J Med Chem*. 49 (2006), 3774-3789.
- [16] B.G. Szczepankiewicz, G. Liu, P.J. Hajduk, C. Abad-Zapatero, Z. Pei, Z. Xin, T.H. Lubben, J.M. Trevillyan, M.A. Stashko, S.J. Ballaron, H. Liang, F. Huang, C.W. Hutchins, S.W. Fesik, M.R. Jirousek. Discovery of a Potent, Selective Protein Tyrosine Phosphatase 1B Inhibitor Using a Linked-Fragment Strategy. *J Am Chem Soc*. 125 (2003), 4087-4096.
- [17] V.M. Balaramnavar, R. Srivastava, N. Rahuja, S. Gupta, A.K. Rawat, S. Varshney, H. Chandasana, Y.S. Chhonker, P.K. Doharey, S. Kumar, S. Gautam, S.P. Srivastava, R.S. Bhatta, J.K. Saxena, A.N. Gaikwad, A.K. Srivastava, A.K. Saxena. Identification of novel PTP1B inhibitors by pharmacophore based virtual screening, scaffold hopping and docking. *Eur J Med Chem*. 87 (2014), 578-594.
- [18] T.N. Doman, S.L. McGovern, B.J. Witherbee, T.P. Kasten, R. Kurumbail, W.C. Stallings, D.T. Connolly, B.K. Shoichet. Molecular Docking and High-Throughput Screening for Novel Inhibitors of Protein Tyrosine Phosphatase-1B. *J Med Chem*. 45 (2002), 2213-2221.
- [19] C. Dufresne, P. Roy, Z. Wang, E. Asante-Appiah, W. Cromlish, Y. Boie, F. Forghani, S. Desmarais, Q. Wang, K. Skorey, D. Waddleton, C. Ramachandran, B.P. Kennedy, L. Xu, R. Gordon, C.C. Chan, Y. Leblanc. The development of potent non-peptidic PTP-1B inhibitors.

- Bioorg Med Chem Lett. 14 (2004), 1039-1042.
- [20] G. Liu, Z. Xin, Z. Pei, P.J. Hajduk, C. Abad-Zapatero, C.W. Hutchins, H. Zhao, T.H. Lubben, S.J. Ballaron, D.L. Haasch, W. Kaszubska, C.M. Rondinone, J.M. Trevillyan, M.R. Jirousek. Fragment screening and assembly: a highly efficient approach to a selective and cell active protein tyrosine phosphatase 1B inhibitor. *J Med Chem.* 46 (2003), 4232-4235.
- [21] B. Douty, B. Wayland, P.J. Ala, M.J. Bower, J. Pruitt, L. Bostrom, M. Wei, R. Klabe, L. Gonneville, R. Wynn, T.C. Burn, P.C. Liu, A.P. Combs, E.W. Yue. Isothiazolidinone inhibitors of PTP1B containing imidazoles and imidazolines. *Bioorg Med Chem Lett.* 18 (2008), 66-71.
- [22] R.B. Sparks, P. Polam, W. Zhu, M.L. Crawley, A. Takvorian, E. McLaughlin, M. Wei, P.J. Ala, L. Gonneville, N. Taylor, Y. Li, R. Wynn, T.C. Burn, P.C. Liu, A.P. Combs. Benzothiazole benzimidazole (S)-isothiazolidinone derivatives as protein tyrosine phosphatase-1B inhibitors. *Bioorg Med Chem Lett.* 17 (2007), 736-740.
- [23] C. Seo, J.H. Sohn, H. Oh, B.Y. Kim, J.S. Ahn. Isolation of the protein tyrosine phosphatase 1B inhibitory metabolite from the marine-derived fungus *Cosmospora* sp. SF-5060. *Bioorg Med Chem Lett.* 19 (2009), 6095-6097.
- [24] X. Fan, N.J. Xu, J.G. Shi. Bromophenols from the Red Alga *Rhodomela confervoides*. *J Nat Prod.* 66 (2003), 455-458.
- [25] R.R. Baumgartner, D. Steinmann, E.H. Heiss, A.G. Atanasov, M. Ganzera, H. Stuppner, V.M. Dirsch. Bioactivity-Guided Isolation of 1,2,3,4,6-Penta-O-galloyl-d-glucopyranose from *Paeonia lactiflora* Roots As a PTP1B Inhibitor. *J Nat Prod.* 73 (2010), 1578-1581.
- [26] D. Shi, J. Li, B. Jiang, S. Guo, H. Su, T. Wang. Bromophenols as inhibitors of protein tyrosine phosphatase 1B with antidiabetic properties. *Bioorg Med Chem Lett.* 22 (2012), 2827-2832.
- [27] B. Jiang, D. Shi, Y. Cui, S. Guo. Design, synthesis, and biological evaluation of bromophenol derivatives as protein tyrosine phosphatase 1B inhibitors. *Arch Pharm (Weinheim).* 345 (2012), 444-453.
- [28] B. Jiang, S. Guo, D. Shi, C. Guo, T. Wang. Discovery of novel bromophenol 3,4-dibromo-5-(2-bromo-3,4-dihydroxy-6-(isobutoxymethyl)benzyl)benzene-1,2-diol as protein tyrosine phosphatase 1B inhibitor and its anti-diabetic properties in C57BL/KsJ-db/db mice. *Eur J Med Chem.* 64 (2013), 129-136.
- [29] D. Shi, S. Guo, B. Jiang, C. Guo, T. Wang, L. Zhang, J. Li. HPN, a Synthetic Analogue of Bromophenol from Red Alga *Rhodomela confervoides*: Synthesis and Anti-Diabetic Effects in C57BL/KsJ-db/db Mice. *Marine Drugs.* 11 (2013), 350-362.
- [30] N. Wu, J. Luo, B. Jiang, L. Wang, S. Wang, C. Wang, C. Fu, J. Li, D. Shi. Marine Bromophenol Bis (2,3-Dibromo-4,5-dihydroxy-phenyl)-methane Inhibits the Proliferation, Migration, and Invasion of Hepatocellular Carcinoma Cells via Modulating β 1-Integrin/FAK Signaling. *Marine Drugs.* 13 (2015), 1010-1025.
- [31] Y. Cui, D. Shi, Z. Hu. Synthesis and protein tyrosine phosphatase 1B inhibition activities of two new synthetic bromophenols and their methoxy derivatives. *Chinese Journal of Oceanology and Limnology.* 29 (2011), 1237-1242.
- [32] M.T. Engström, M. Karonen, J.R. Ahern, N. Baert, B. Payré, H. Hoste, J.P. Salminen. Chemical Structures of Plant Hydrolyzable Tannins Reveal Their in Vitro Activity against Egg Hatching and Motility of *Haemonchus contortus* Nematodes. *J Agr Food Chem.* 64 (2016), 840-851.

- [33] C. Xu, Y. Yagiz, W. Hsu, A. Simonne, J. Lu, M.R. Marshall. Antioxidant, Antibacterial, and Antibiofilm Properties of Polyphenols from Muscadine Grape (*Vitis rotundifolia* Michx.) Pomace against Selected Foodborne Pathogens. *J Agr Food Chem.* 62 (2014), 6640-6649.
- [34] C. Huang, S. Lee, C. Lin, T. Tu, L.H. Chen, Y.J. Chen, H. Huang. Co-treatment with Quercetin and 1,2,3,4,6-Penta-O-galloyl- β -D-glucose Causes Cell Cycle Arrest and Apoptosis in Human Breast Cancer MDA-MB-231 and AU565 Cells. *J Agr Food Chem.* 61 (2013), 6430-6445.
- [35] V.C. Lin, P. Kuo, Y. Lin, Y. Chen, Y. Hseu, H. Yang, J. Kao, C. Ho, T. Way. Penta-O-galloyl- β -D-glucose Suppresses EGF-Induced eIF3i Expression through Inhibition of the PI3K/AKT/mTOR Pathway in Prostate Cancer Cells. *J Agr Food Chem.* 62 (2014), 8990-8996.
- [36] L.T.M. Ngan, J. Moon, T. Shibamoto, Y. Ahn. Growth-Inhibiting, Bactericidal, and Urease Inhibitory Effects of *Paeonia lactiflora* Root Constituents and Related Compounds on Antibiotic-Susceptible and -Resistant Strains of *Helicobacter pylori*. *J Agr Food Chem.* 60 (2012), 9062-9073.
- [37] Z. Xin, G. Liu, C. Abad-Zapatero, Z. Pei, B.G. Szczepankiewicz, X. Li, T. Zhang, C.W. Hutchins, P.J. Hajduk, S.J. Ballaron, M.A. Stashko, T.H. Lubben, J.M. Trevillyan, M.R. Jirousek. Identification of a monoacid-based, cell permeable, selective inhibitor of protein tyrosine phosphatase 1B. *Bioorg Med Chem Lett.* 13 (2003), 3947-3950.
- [38] Y. Wei, Y. Chen, L. Shi, L. Gao, S. Liu, Y. Cui, W. Zhang, Q. Shen, J. Li, F. Nan. Discovery and structural modification of novel inhibitors of PTP1B inspired by the ACT fragment of scleritodermin A. *MedChemComm.* 2 (2011), 1104.
- [39] L.F. Iversen. Structure Determination of T Cell Protein-tyrosine Phosphatase. *J Biol Chem.* 277 (2002), 19982-19990.
- [40] The structure of internal standard was showed in supporting information.
- [41] M. Patra, T.C. Johnstone, K. Suntharalingam, S.J. Lippard. A Potent Glucose-Platinum Conjugate Exploits Glucose Transporters and Preferentially Accumulates in Cancer Cells. *Angew Chem Int Ed Engl.* 55 (2016), 2550-2554.

- the hybrid of bromophenol and saccharide was prepared
- compound **10a** exhibited remarkable selectivity for PTP1B over TCPTP
- molecule docking and molecular dynamics studies reveal the reason of selectivity
- the cell permeability and cellular activity of compound **10a** were demonstrated

ACCEPTED MANUSCRIPT